Polaritons and Pairing Phenomena in Bose-Hubbard Mixtures

M. J. Bhaseen, M. Hohenadler,* A. O. Silver, and B. D. Simons

Cavendish Laboratory, University of Cambridge, Cambridge, CB3 0HE, United Kingdom
(Received 23 December 2008; published 30 March 2009)

Motivated by recent experiments on cold atomic gases in ultrahigh finesse optical cavities, we consider the two-band Bose-Hubbard model coupled to quantum light. Photoexcitation promotes carriers between the bands, and we study the interplay between Mott insulating behavior and superfluidity. The model displays a U(1) × U(1) symmetry which supports the coexistence of Mott insulating and superfluid phases and yields a rich phase diagram with multicritical points. This symmetry is shared by several other problems of current experimental interest, including two-component Bose gases in optical lattices and the bosonic BEC-BCS crossover for atom-molecule mixtures induced by a Feshbach resonance. We corroborate our findings by numerical simulations.

Introduction.—The spectacular advances in cold atomic gases have led to landmark experiments in strongly correlated systems. With the observation of the superfluid–Mott-insulator transition in ^{87}Rb [1] and the BEC-BCS crossover in ^{40}K [2], attention is now being directed towards multicomponent gases. Whether they be distinct atoms or internal states, such systems bring "isospin" degrees of freedom. They offer the fascinating prospect to realize novel phases and to study quantum magnetism, Mott physics, and superfluidity [3].

More recently, significant experimental progress has been made in combining cavity quantum electrodynamics (cavity QED) with ultracold gases. Strong atom-field coupling has been achieved using ultrahigh finesse optical cavities [4] and with optical fibers on atom chips [5]. These experiments open an exciting new chapter in coherent matter-light interaction and have already led to pioneering studies of condensate dynamics [6]. The light field serves not only as a probe of the many-body system but may also support interesting cavity-mediated phenomena and phases. This dual role has been exploited in studies of polariton condensates in semiconductor microcavities [7]. It is reinforced by ground-breaking cavity QED experiments using superconducting qubits in microwave resonators [8]. This has led to solid state measurements of the collective states of the Dicke model [9] and remarkable observations of the Lamb shift [10].

In this work, we examine the impact of cavity radiation on the Bose-Hubbard model. We focus on a two-band model in which photons induce transitions between two internal states or Bloch bands. This is a natural generalization of the much studied two-level systems coupled to radiation and may serve as a useful paradigm in other contexts. The new ingredients are that the bosonic carriers may form a Mott insulator or indeed condense. The primary question is whether a novel Mott insulating state can survive, which supports a condensate of photoexcitations or mobile defects. In analogy with zero point motion in helium [11], this may be viewed as a form of supersolid in

which fluctuations of the photon field induce defects. While this question has its origin in polariton condensates in fermionic band insulators [12], the present problem is rather different. Since the integrity of the Mott state is tied to the interactions, *a priori* it is unclear that it survives the effects of itinerancy and photoexcitation. Nonetheless, the outcome is affirmative, and the model displays both this novel phase and a rich phase diagram. Related phases were recently observed in simulations of other two-component models [13,14].

The model.—Let us consider a two-band Bose-Hubbard model coupled to the light field of an optical cavity within the rotating wave approximation

$$H_0 = \sum_{i\alpha} \epsilon_\alpha n_i^\alpha + \sum_{i\alpha} \frac{U_\alpha}{2} n_i^\alpha (n_i^\alpha - 1) + V \sum_i n_i^a n_i^b$$
$$- \sum_{\langle ij\rangle\alpha} J_\alpha \alpha_i^\dagger \alpha_j + \omega \psi^\dagger \psi + g \sum_i (b_i^\dagger a_i \psi + \text{H.c.}), \quad (1)$$

where $\alpha = a, b$ are two bands of bosons with $[\alpha_i, \alpha_j^\dagger] = \delta_{ij}$. These might be states of different orbital or spin angular momentum. Here, ϵ_α effects the band splitting, U_α and V are interactions, J_α are nearest-neighbor hopping parameters, and ω is the frequency of the mode ψ. We consider just a single mode, which couples uniformly to the bands. The coupling g is the strength of the matter-light interaction. In view of the box normalization of the photon, we denote $g \equiv \bar{g}/\sqrt{N}$, where N is the number of lattice sites. It is readily seen that $N_1 = \sum_i (n_i^b + n_i^a)$ and $N_2 = \psi^\dagger \psi + \sum_i (n_i^b - n_i^a + 1)/2$ commute with H_0. These are the total number of atomic carriers and photoexcitations (or polaritons), respectively. These conservation laws reflect the global U(1) × U(1) symmetry of H_0, such that $a \rightarrow e^{i\vartheta} a$, $b \rightarrow e^{i\varphi} b$, and $\psi \rightarrow e^{-i(\vartheta - \varphi)} \psi$, where ϑ and φ are arbitrary. This symmetry will have a direct manifestation in the phase diagram and suggests implications for other multicomponent problems. We begin by assuming that a are strongly interacting hard-core bosons and that b are dilute so that we may neglect their interactions.

Zero hopping limit.—To gain insight into (1), we examine the zero hopping limit. This will anchor the phase diagram to an exactly solvable many-body limit. The photon couples all of the sites and in the thermodynamic limit is described by a coherent state $|\gamma\rangle \equiv e^{-(\gamma^2/2)}e^{\gamma\psi^\dagger}|0\rangle$, with mean occupation $\langle\psi^\dagger\psi\rangle = \gamma^2$. We may replace the grand canonical Hamiltonian $H \equiv H_0 - \mu_1 N_1 - \mu_2 N_2$ by an effective single site problem $\langle\gamma|H|\gamma\rangle \equiv \sum_i \mathcal{H}_i$:

$$\mathcal{H} \equiv \sum_\alpha \tilde{\epsilon}_\alpha n_\alpha + \tilde{\omega}\bar{\gamma}^2 + \bar{g}\,\bar{\gamma}(b^\dagger a + a^\dagger b), \qquad (2)$$

and we drop the offset $-\mu_2/2$. We define $\tilde{\epsilon}_a \equiv \epsilon_a - \mu_1 + \mu_2/2$, $\tilde{\epsilon}_b \equiv \epsilon_b - \mu_1 - \mu_2/2$, $\tilde{\omega} \equiv \omega - \mu_2$, and the mean photon occupation per site $\bar{\gamma}^2 \equiv \gamma^2/N$. The effective Hamiltonian (2) describes a single two-level system coupled to an effective "radiation field" of b particles, or the Jaynes-Cummings model; for N two-level systems, this is known as the Dicke or Tavis-Cummings model and is integrable [15,16]. These paradigmatic models are well known in both atomic physics and quantum optics and describe localized excitons coupled to light [12]. The eigenstates of (2) are superpositions in the upper and lower bands (that we denote as $|0, n\rangle$ and $|1, n-1\rangle$, respectively) with total occupancy n. The lowest energy is $E_n^- = \tilde{\omega}\bar{\gamma}^2 + n\tilde{\epsilon}_b - \tilde{\omega}_0/2 - \sqrt{\tilde{\omega}_0^2/4 + \bar{g}^2\bar{\gamma}^2 n}$, where $\tilde{\omega}_0 \equiv \tilde{\epsilon}_b - \tilde{\epsilon}_a$. Minimizing on $\bar{\gamma}$ gives a self-consistency equation for the photon, and the resulting eigenstates yield the zero hopping phase diagram in Fig. 1. In the thermodynamic limit described here, only the lowest Mott state, with $n_a + n_b = 1$, survives; for $\mu_1 \geq \epsilon_b - \mu_2/2 - \bar{g}^2/4\tilde{\omega}$, it is favorable to macroscopically populate the upper band. Within this stable Mott phase, the variation yields either $\bar{\gamma} = 0$, corresponding to zero photon occupancy, or $\bar{\gamma}^2 = (\bar{g}^4 - \bar{g}_c^4)/4\tilde{\omega}^2\bar{g}^2$, where $\bar{g}_c \equiv \sqrt{\tilde{\omega}\tilde{\omega}_0}$; the former occurs for $\bar{g} \leq \bar{g}_c$ and the latter for $\bar{g} \geq \bar{g}_c$. In fact, this onset corresponds to the superradiance transition in the Dicke model [15,16]. Indeed, since $n_a + n_b = 1 \equiv 2S$ in the lowest lobe, one may construct the Dicke model directly from (1) by using a spin $S = 1/2$ Schwinger boson representation, where $S^+ \equiv b^\dagger a$, $S^- \equiv a^\dagger b$, and $S^z \equiv (n_b - n_a)/2$:

$$H = \tilde{\omega}_0 \sum_i S_i^z + \tilde{\omega}\psi^\dagger\psi + g\sum_i(S_i^\dagger\psi + \text{H.c.}). \qquad (3)$$

This describes N two-level systems (or spins) coupled to photons and may be treated using *collective* spins $\mathbf{J} \equiv \sum_i^N \mathbf{S}_i$. This yields a large effective spin, which may be treated semiclassically as $N \to \infty$. The onset of the photon is accompanied by a magnetization $\mathcal{M} \equiv \langle J^z\rangle/N$, which also serves as an order parameter for this continuous transition: $\mathcal{M} = -1/2$, for $\bar{g} \leq \bar{g}_c$, and $\mathcal{M} = -(\bar{g}_c/\bar{g})^2/2$, for $\bar{g} \geq \bar{g}_c$. This growth reflects the population imbalance $\langle n_b\rangle - \langle n_a\rangle$ due to photoexcitations. The agreement between the variational and Dicke model results is a useful platform for departures.

Variational phase diagram.—Having confirmed a zero hopping Mott phase, with $n_a + n_b = 1$, let us consider
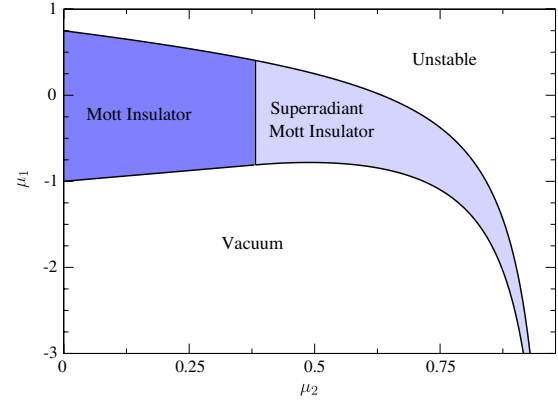
FIG. 1 (color online). Zero hopping phase diagram in the large-U_a limit, with $\epsilon_b = -\epsilon_a = \omega = \bar{g} = 1$, corresponding to $\omega < \omega_0$. The vertical line $\bar{g} = \bar{g}_c$ is the superradiance transition in the Dicke model and separates a Mott insulator with $n_a + n_b = 1$ and $\langle\psi^\dagger\psi\rangle = 0$ (dark blue) from a superradiant Mott insulator with $\langle\psi^\dagger\psi\rangle \neq 0$ (light blue). Outside are the vacuum and an unstable region corresponding to macroscopic population of the b states. While the total density is fixed within both Mott phases, the individual a and b populations vary in the superradiant phase and may be viewed as isospin order. For $\omega > \omega_0$, the boundaries may cross and terminate the lobe.

itinerancy and carrier superfluidity. Within this lowest lobe, we may consider *hard-core a and b* bosons [17]. A convenient approach is to augment the variational analysis of Ref. [3] with a coherent state for the light field:

$$|\mathcal{V}\rangle = |\gamma\rangle \otimes \prod_i [\cos\theta_i(\cos\chi_i a_i^\dagger + \sin\chi_i b_i^\dagger)$$
$$+ \sin\theta_i(\cos\eta_i + \sin\eta_i b_i^\dagger a_i^\dagger)]|0\rangle, \qquad (4)$$

where $|\gamma\rangle$ is the coherent state introduced previously and θ, χ, η, and γ are to be determined. The first term in brackets describes the Mott state, and the second superfluidity. For $\theta = 0$ this coincides with the variational approach for localized excitons coupled to light [12] and reproduces the previous results for $J_\alpha = 0$. More generally, (4) takes into account the effects of real hopping, involving site vacancies and interspecies double occupation. It provides a starting point to identify the boundaries between the Mott-insulator and superfluid regions. We consider spatially uniform phases, with energy density $\mathcal{E} \equiv \langle\mathcal{V}|H|\mathcal{V}\rangle/N$:

$$\mathcal{E} = (\tilde{\epsilon}_+ - \tilde{\epsilon}_- \cos 2\chi)\cos^2\theta + (2\tilde{\epsilon}_+ + V)\sin^2\eta\sin^2\theta$$
$$- \frac{z}{4}[J_a\cos^2(\chi - \eta) + J_b\sin^2(\chi + \eta)]\sin^2 2\theta$$
$$+ \tilde{\omega}\bar{\gamma}^2 + \bar{g}\,\bar{\gamma}\cos^2\theta\sin 2\chi, \qquad (5)$$

where z is the coordination number and $\tilde{\epsilon}_\pm \equiv (\tilde{\epsilon}_b \pm \tilde{\epsilon}_a)/2$. Minimizing on $\bar{\gamma}$ yields $\bar{\gamma} = -\bar{g}\cos^2\theta\sin 2\chi/2\tilde{\omega}$, and one may eliminate this from $\mathcal{E}$. Exploiting symmetries, one may minimize $\mathcal{E}$ over $[0, \pi/2]$. The order parameters $\langle a\rangle = \frac{1}{2}\sin 2\theta\cos(\chi - \eta)$, $\langle b\rangle = \frac{1}{2}\sin 2\theta\sin(\chi + \eta)$, and

$\langle \psi^\dagger \psi \rangle / N = \bar{\gamma}^2$ yield the phase diagram in Fig. 2, where $J_a = J_b = J$. For the chosen parameters, we have four distinct phases: (i) a Mott state with $\langle a \rangle = \langle b \rangle = \langle \psi^\dagger \psi \rangle = 0$, (ii) a superradiant Mott state with $\langle a \rangle = \langle b \rangle = 0$ and $\langle \psi^\dagger \psi \rangle \neq 0$, (iii) a single component superfluid with $\langle a \rangle \neq 0$ and $\langle b \rangle = \langle \psi^\dagger \psi \rangle = 0$, and (iv) a superradiant superfluid with $\langle a \rangle \neq 0$, $\langle b \rangle \neq 0$, and $\langle \psi^\dagger \psi \rangle \neq 0$. Indeed, the Hamiltonian displays a U(1) × U(1) symmetry, and these may be broken independently. The phase diagram reflects this pattern of symmetry breaking. In particular, the superradiant Mott state corresponds to an unbroken U(1) in the matter sector (corresponding to a pinned density and phase fluctuations) but a broken U(1) (or phase coherent condensate) for photoexcitations. The expectation value of the *bilinear* $\langle b^\dagger a \rangle \neq 0$ corresponds to the onset of coherence in the Dicke model. This novel phase may be regarded as a form of supersolid.

In the absence of competition from other phases, the transition between the nonsuperradiant insulator ($\theta = \chi = \bar{\gamma} = 0$) and the a-type superfluid ($\theta \neq 0$, $\chi = \eta = \bar{\gamma} = 0$) occurs when $\tilde{\epsilon}_a + zJ = 0$. In Fig. 2, this is the line $\mu_2 = 2(1 - zJ)$. This crosses the superradiance boundary at a tetracritical point $(zJ^c, \mu_2^c) = (r/2, 2 - r)$, where $r \equiv (1 + \sqrt{5})/2$ is the golden ratio. This follows from a Landau expansion of (5); eliminating $\bar{\gamma}$, all the quadratic "mass" terms vanish. More generally, the phase diagram evolves with the parameters, and the a-type superfluid may be replaced by the proximate phases [18].

Numerical simulations.—To corroborate our findings, we perform exact diagonalization on a 1D system of hard-core a and b bosons, with $N = 8$ sites and periodic boundary conditions. The Hilbert space is truncated to a maximum number of photons $M_\psi = 2N = 16$. Figure 3

shows the total atom, photon, a-atom, and b-atom density. The dashed lines indicate the approximate locations of the Mott-insulator–superfluid (vertical line) and superradiance (horizontal line) transitions, as determined from (a) and (b). Although an accurate phase diagram for the thermodynamic limit is beyond the scope of this work, the features are in excellent agreement with Fig. 2. This parallels the success of mean field theory in other low-dimensional bosonic systems and is remarkable given the enhanced role of fluctuations. This may be assisted by the long range nature of the cavity photons. The superradiance transition encompasses the superfluid and Mott phases and yields a tetracritical point; see (a) and (b). In addition, the region of a density overextends that of b density resulting in a pure
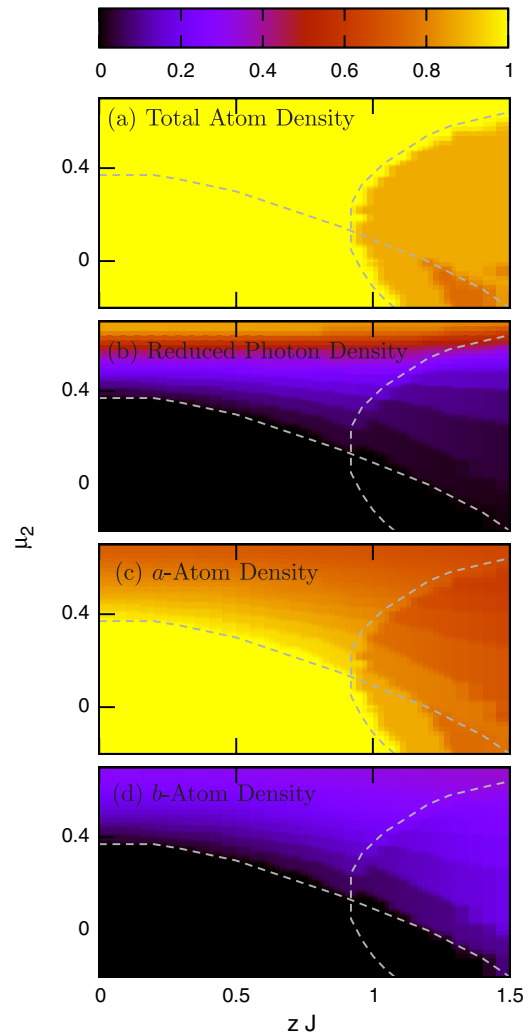
FIG. 3 (color online). Exact diagonalization for a 1D system with 8 sites, $M_\psi = 16$ photons, and the parameters of Fig. 2. We show (a) the total atom density and the Mott-insulator–superfluid transition, (b) the density of photons (reduced by a factor of 2) and the onset of superradiance, (c) the density of a atoms, and (d) the density of b atoms. The dashed lines are a guide to the eye and indicate the Mott-insulator–superfluid and superradiance transitions, as determined by hand from (a) and (b). Their intersection yields the location of the tetracritical point.

FIG. 2 (color online). Variational phase diagram with $J_a = J_b = J$, $\epsilon_a = -1$, $\epsilon_b = 1$, $\omega = V = \bar{g} = 1$, and $\mu_1 = 0$. The phases are (i) a Mott insulator (dark blue), (ii) a superradiant Mott state supporting a condensate of photoexcitations (light blue), (iii) a superradiant superfluid (light red), and (iv) an a-type superfluid (dark red). The circles denote the transition to superfluidity as determined by θ, and the squares denote the onset of photons as determined by χ. For these parameters, the transition from the Mott insulator to the superradiant Mott state occurs for $\mu_2^c = (3 - \sqrt{5})/2 \approx 0.382$.

a-type superfluid; see (c) and (d). Our simulations suggest that this phase is stable with increasing system size [18].

Discussion.—A feature not addressed by the present mean field theory, but captured in Fig. 3, is the dispersion of the superradiance transition with J; in the Mott phase, $\theta = 0$, and J drops out of the variational energy (5). One way to understand this is to recast the matter contribution as $|\mathcal{V}_M\rangle = \prod_i (\cos\chi_i + \sin\chi_i b_i^\dagger a_i)|\Omega\rangle$, where $|\Omega\rangle \equiv \prod_i a_i^\dagger |0\rangle$. This accommodates only *local* particle-hole pairs. By analogy with the BCS approach to exciton insulators [19], the Mott state may be refined and the J dependence restored by incorporating momentum space pairing [18]. This connection to the BEC-BCS crossover for bosons [20] is reinforced by the Feshbach resonance problem studied in the absence of a lattice [21–23]. Performing a particle-hole transformation, the matter-light coupling reads $\psi^\dagger a_i b_i$. Aside from the global nature of the photon, this converts a and b into a "molecule" ψ. At the outset there are eight phases corresponding to condensation of $\langle a \rangle$, $\langle b \rangle$, and $\langle \psi \rangle$. Of these, only five may survive; condensation of two variables provides an effective field (as dictated by the coupling) which induces condensation of the other. The band asymmetry $\epsilon_a < \epsilon_b$ reduces this to four, or less, depending on the parameters. In contrast to the single species mean field theory, this case supports an atomic superfluid, since condensation of one carrier no longer induces a field. Moreover, condensation may leave a U(1) symmetry intact, which allows the coexistence of Mott insulating and phase coherent behavior.

In deriving (5) and the phase diagram, we are primarily concerned with the matter-light coupling. As such, we incorporate V as in Ref. [3]. This gives rise to the nontrivial phases in Fig. 2. However, as noted by Söyler *et al.* [13], analogous phases may be stabilized in the two-component Bose-Hubbard model, *without* matter-light coupling, through a more sophisticated treatment of V itself. Indeed, on site repulsive interactions $V n_a n_b$ favor a particle of one species and a hole of the other on the same site. Treating this pairing in a BCS approach, one may replace $n_i^a n_i^b$ by $|\Delta_i|^2 + (\Delta_i b_i^\dagger a_i + \text{H.c.})$, where $\Delta_i \equiv \langle a_i^\dagger b_i \rangle$ is to be determined self-consistently. This field acts as a *local* "photon," and a similar mean field phenomenology may ensue. Such pairing also occurs in fermionic models [24]. Although our discussion has focused on a single *global* photon, the symmetry analysis is more general. This is supported by studies of the two-band Bose-Hubbard model for equal fillings and commensurate densities [25]. We shall provide details of the similarities and differences of this local problem in Ref. [18]. The classical limit may also be realized in optical superlattices, where $g_i a_i b_i^\dagger$ is tunneling between wells a and b.

Conclusions.—We have considered the impact of photoexcitations on the Bose-Hubbard model. The phase diagram supports a novel phase where photoexcitations condense on the background of a Mott insulator. We have performed numerical simulations and highlighted connec-tions to other problems of current interest. Directions for research include the impact of fluctuations and the nature of collective excitations. It would also be interesting to incorporate a finite photon wave vector. This may stabilize inhomogeneous phases and probe incommensurate magnetism. Recent studies of Bose-Fermi mixtures also display a similar phenomenology, in which superfluidity is replaced by fermionic metallicity [26].

*Present address: OSRAM Opto Semiconductors GmbH, 93055 Regensburg, Germany.
[1] M. Greiner *et al.*, Nature (London) **415**, 39 (2002).
[2] C. A. Regal, M. Greiner, and D. S. Jin, Phys. Rev. Lett. **92**, 040403 (2004).
[3] E. Altman, W. Hofstetter, E. Demler, and M. D. Lukin, New J. Phys. **5**, 113 (2003).
[4] F. Brennecke *et al.*, Nature (London) **450**, 268 (2007).
[5] Y. Colombe *et al.*, Nature (London) **450**, 272 (2007).
[6] F. Brennecke, S. Ritter, T. Donner, and T. Esslinger, Science **322**, 235 (2008).
[7] J. Kasprzak *et al.*, Nature (London) **443**, 409 (2006).
[8] A. Wallraff *et al.*, Nature (London) **431**, 162 (2004).
[9] J. M. Fink *et al.*, arXiv:0812.2651.
[10] A. Fragner *et al.*, Science **322**, 1357 (2008).
[11] A. F. Andreev and I. M. Lifshitz, Sov. Phys. JETP **29**, 1107 (1969).
[12] P. B. Littlewood *et al.*, J. Phys. Condens. Matter **16**, S3597 (2004).
[13] S. G. Söyler, B. Capogrosso-Sansone, N. V. Prokof'ev, and B. V. Svistunov, arXiv:0811.0397.
[14] V. G. Rousseau and P. J. H. Denteneer, Phys. Rev. Lett. **102**, 015301 (2009).
[15] R. H. Dicke, Phys. Rev. **93**, 99 (1954).
[16] K. Hepp and E. H. Lieb, Ann. Phys. (N.Y.) **76**, 360 (1973).
[17] While this does not affect physics *within* the lobe, the upper boundary is modified by the possible b population.
[18] M. J. Bhaseen, M. Hohenadler, A. O. Silver, and B. D. Simons (to be published).
[19] L. V. Keldysh and Y. V. Kopaev, Sov. Phys. Solid State **6**, 2219 (1965).
[20] A. Koetsier, P. Massignan, R. A. Duine, and H. T. C. Stoof, arXiv:0809.4189.
[21] L. Radzihovsky, J. Park, and P. B. Weichman, Phys. Rev. Lett. **92**, 160402 (2004).
[22] M. W. J. Romans, R. A. Duine, S. Sachdev, and H. T. C. Stoof, Phys. Rev. Lett. **93**, 020405 (2004).
[23] L. Zhou *et al.*, Phys. Rev. A **78**, 053612 (2008).
[24] A. Kantian, A. J. Daley, P. Törmä, and P. Zoller, New J. Phys. **9**, 407 (2007).
[25] A. Kuklov, N. Prokof'ev, and B. Svistunov, Phys. Rev. Lett. **92**, 050402 (2004).
[26] S. Sinha and K. Sengupta, arXiv:0811.4515.